

# Green CO<sub>2</sub> technology for the preparation of aerogel dry powder loaded with beclomethasone dipropionate

Thoa Duong<sup>a</sup>, Clara López-Iglesias<sup>a</sup>, Annalisa Bianchera<sup>b</sup>, Maria Vivero-Lopez<sup>a</sup>, Inés Ardao<sup>c</sup>, Ruggero Bettini<sup>b</sup>, Carmen Alvarez-Lorenzo<sup>a</sup>, Carlos A. García-González<sup>a,\*</sup>

<sup>a</sup> AerogelsLab, I+D Farma Group (GI-1645), Department of Pharmacology, Pharmacy and Pharmaceutical Technology, Faculty of Pharmacy, iMATUS and Health Research Institute of Santiago de Compostela (IDIS), Universidade de Santiago de Compostela, Santiago de Compostela E-15782, Spain

<sup>b</sup> Food and Drug Department, University of Parma, Parco Area delle Scienze 27/A, Parma 43124, Italy

<sup>c</sup> BioFarma Research group, Department of Pharmacology, Pharmacy and Pharmaceutical Technology, Innopharma Drug Screening and Pharmacogenomics Platform, Centro Singular de Investigación en Medicina Molecular y Enfermedades Crónicas (CIMUS) and Health Research Institute of Santiago de Compostela (IDIS), Universidade de Santiago de Compostela, Santiago de Compostela E-15782, Spain

## ARTICLE INFO

### Keywords:

Green technology  
Supercritical CO<sub>2</sub>  
Dry powder inhalers  
Beclomethasone dipropionate  
Drug-loaded aerogel

## ABSTRACT

Dry powder inhalers (DPIs) have gained increasing clinical acceptance in the local treatment of lung diseases due to their ability to meet the evolving needs of patients while avoiding environmental concerns. However, some formulations for DPIs still encounter performance limitations in terms of aerodynamic properties and achievement of therapeutic doses. Innovative aerogel powder formulations for DPIs processed using combined supercritical CO<sub>2</sub> (scCO<sub>2</sub>)-based technologies can overcome these limitations, especially in the case of poorly water-soluble drugs. The loading of hydrophobic drugs into aerogels can be optimized through a thorough understanding of the physicochemical properties of the formulation and the scCO<sub>2</sub> processing conditions. In this study, drug-loaded alginate aerogel particles were prepared by combining gelation-emulsification techniques and scCO<sub>2</sub>-based technologies. Beclomethasone dipropionate (BDP), a hydrophobic corticosteroid, was incorporated into the aerogel matrix by scCO<sub>2</sub> impregnation. The influence of contact time, initial amount of drug, and use of co-solvents on the efficiency of scCO<sub>2</sub> impregnation were studied. The kinetics of the BDP adsorption process was modelled to elucidate the time required for the drug to attain equilibrium concentration under specific operating conditions. Nitrogen adsorption-desorption and helium pycnometry revealed particles with large surface area (>200 m<sup>2</sup>/g) and porosity (ca. 90%). The resulting aerogels had excellent aerodynamic properties at relevant BDP doses, as confirmed by *in vitro* lung deposition tests. *Ex vivo* permeability tests with porcine lung tissues evidenced that BDP released from the inhaled formulation could penetrate the bronchial tissue.

## 1. Introduction

Pulmonary drug delivery is primarily used for the local treatment of lung diseases, as it minimizes systemic side effects and improves patient adherence [1],[2]. Dry powder inhalers (DPIs) have gained prominence and increasing market demand as devices for pulmonary drug delivery due to their eco-friendliness, ease of use, stability of the formulation, and wide potential for treating respiratory conditions [3],[4]. However, DPIs encounter challenges to deliver therapeutic drug concentrations to the desired regions within the lungs, often due to lung defense mechanisms, and systemic absorption resulting from particle deposition in the mouth or oropharynx due to the deficient aerodynamic properties.

Significant efforts have been directed towards novel particle engineering for optimizing DPIs performance [5]. Among them, porous formulations are especially promising since they present very low particle density associated with a higher surface area that improves their aerodynamic behavior. However, only a few pioneering powder technologies, like Pulmosphere™, Technosphere®, and ARCUS technologies, have gained approval for commercial use [5],[6]. Finally, these challenges to design DPI formulations are further amplified when dealing with drugs that exhibit poor solubility in water [7],[8],[9].

Beclomethasone dipropionate (BDP) is an extremely poorly water-soluble (<1 µg/mL in water) anti-inflammatory prodrug commonly prescribed for asthma patients [9],[10], which is converted in the lung

\* Corresponding author.

E-mail address: [carlos.garcia@usc.es](mailto:carlos.garcia@usc.es) (C.A. García-González).

<https://doi.org/10.1016/j.jcou.2024.102722>

Received 8 January 2024; Received in revised form 11 February 2024; Accepted 25 February 2024

Available online 2 March 2024

2212-9820/© 2024 The Author(s). Published by Elsevier Ltd. This is an open access article under the CC BY license (<http://creativecommons.org/licenses/by/4.0/>).

to the active metabolite beclomethasone 17-monopropionate by the action of esterases [11]. Currently, commercial products incorporating BDP are available in DPIs, such as Easyhaler (Orion Pharma Ltd., London, UK) [12] and Fostair NEXThaler (Chiesi Farmaceutici S.p.A, Parma, Italy), which contains a combination of BDP and formoterol fumarate (FF) [13]. Nevertheless, the significantly high content of excipients in the inhaled formulations, e.g. lactose in Fostair NEXThaler (100 µg of BDP, 6 µg FF, and 9.9 mg of lactose monohydrate), might pose challenges for patients using inhalers on a daily basis. Similarly to other potent inhaled corticosteroids, such as fluticasone propionate and mometasone furoate, BDP also has a low nominal dose (less than 1 mg) and an extremely poor water solubility [14]. The use of porous matrices can improve not only the aerodynamic performance of BDP formulations for DPIs, but also the dissolution rate of BDP, due to their high surface area and their capacity to incorporate BDP as solid dispersions [15].

Supercritical fluid (SCF) technologies can be used to produce solid powders for DPI formulations and have been recognized for their cost-effectiveness, non-toxicity, and environmental friendliness [16],[17]. Particularly, CO<sub>2</sub> is a solvent approved by the United States Food and Drug Administration (FDA) and the most common SCF, since it is non-toxic, non-flammable, cost-effective, comes from recycled sources, and has low surface tension and mild critical point conditions (31.1 °C, 73.8 bar) [16],[18],[19]. Namely, the technological platform based on the use of scCO<sub>2</sub> sets several strategies to formulate porous nanostructured powders loaded with drugs of differing water solubility [15],[20],[21]. Among them, aerogels are materials endowed with low bulk density, large surface area and high porosity, which are usually obtained by scCO<sub>2</sub> drying of gels and have been proposed as the next generation of DPI formulations [22],[20]. scCO<sub>2</sub> drying prevents pore collapse of the structure and preserves the physicochemical characteristics of the polymeric gels. Aerogel particles with the right granulometry can compile the aerodynamic and geometrical requirements for pulmonary drug delivery while improving flow dispersibility [23],[24]. Recently, aerogels produced via emulsion or thermal inkjet printing gelation techniques followed by scCO<sub>2</sub> drying have been studied regarding their potential in pulmonary drug delivery [23],[24],[25].

To the best knowledge of the authors, the present study marks the pioneering application of scCO<sub>2</sub>-assisted impregnation for integrating active pharmaceutical ingredients (APIs) into nanostructured aerogels for DPIs. The use of powder technology for inhalable formulations based on BDP-loaded aerogels with potential for industrial scale production is herein studied. The processing method should consider several design aspects – it must be able to simultaneously preserve the physicochemical properties of the aerogel matrix, and to incorporate poorly water-soluble BDP into aerogels. scCO<sub>2</sub>-soluble drugs can be loaded into aerogel matrices by a process known as scCO<sub>2</sub>-assisted impregnation [16],[18],[19]. In this process, the drug molecules dissolved in the supercritical medium effectively penetrate the swollen aerogel matrix and are trapped inside the polymeric structure upon depressurization [26],[27]. However, the low solubility of BDP in scCO<sub>2</sub> presents a significant challenge for its loading by scCO<sub>2</sub>-assisted impregnation. This issue has been previously overcome for other drugs by the addition of polar co-solvents (e.g., ethanol, acetone or methanol) that improve the solubility of the drug in the supercritical medium, thus facilitating the impregnation process [26],[27]. Tuning of other impregnation parameters, such as impregnation contact time or drug:carrier weight ratio, could result in increased loading efficiencies and drug content, hence improving the overall productivity of the process as well as its cost-effectiveness [28].

In this study, the scCO<sub>2</sub> technological platform was applied with a two-fold interest: (i) to dry alginate gel particles prepared through an internal gelation (gelation-emulsification) method (scCO<sub>2</sub> drying), and (ii) to load BDP (scCO<sub>2</sub> impregnation process) into the resulting aerogel particles [29],[30]. The aerogel formulations were then assessed for their drug loading capacity and aerodynamic performance in pulmonary drug delivery for potential use as DPI formulations. The scCO<sub>2</sub>

impregnation procedure was herein developed and the impact of various parameters (impregnation time, drug:carrier ratio, co-solvent choice) was investigated. The textural properties and BDP content of the produced aerogels were determined and used to model the impregnation kinetics. *In vitro* drug release and deposition tests in a compendial impactor were performed to evaluate the therapeutic potential of the optimized BDP-loaded formulation. Lastly, *ex vivo* permeability tests using porcine bronchial tissue were carried out to evaluate the penetration capacity of the aerogels into the bronchial tissue.

## 2. Materials and Methods

### 2.1. Materials

Beclomethasone dipropionate (BDP, > 98% purity) was provided by Tokyo Chemical Industry Co., Ltd (Tokyo, Japan). Alginate acid sodium salt from brown algae (guluronic acid/mannuronic acid ratio of 70/30, M<sub>w</sub> = 403 kDa) was obtained from Sigma Aldrich (Irvine, UK). Calcium chloride (CaCl<sub>2</sub>) was purchased from Merck (Darmstadt, Germany). Carbon dioxide (CO<sub>2</sub> > 99.8% purity) was supplied by Nippon Gases (Madrid, Spain). Acetone (100% purity) was provided by Scharlau Chemie S.A (Barcelona, Spain). Absolute ethanol, methanol (100% purity), Tween 80, and Span 80 were from Merck (Darmstadt, Germany). Paraffin oil was purchased from Carlo Erba Reagents (Emmendingen, Germany). Acetonitrile was supplied from VWR International S.A.S (Rosny-sous-Bois, France).

### 2.2. Preparation of BDP-loaded alginate aerogels

#### 2.2.1. Preparation of alginate gel particles

Alginate aerogels were prepared by a gelation-emulsification method. Briefly, 40 mL of 1.5 % w/v alginate solutions in Milli-Q water were prepared under magnetic stirring (600 rpm) at room temperature. To prepare the oil phase, 3 g of a mixture of Span 80 and Tween 80 (75 and 25 % w/w, respectively) were dissolved into 40 mL of paraffin oil and homogenized by mechanical stirring (1000 rpm, VOS 60 control, VWR) for 10 min. Then, the alginate solution was added drop by drop into the oil phase and the resulting water-in-oil emulsion (1:1 volume ratio) was mechanically stirred for 30 min at 1000 rpm. The velocity of the mechanical stirring was decreased to 600 rpm, the crosslinking solution (6 % w/v CaCl<sub>2</sub>) was then added dropwise, and the emulsion was left to age 2 h. Subsequently, 100 mL of ethanol were added, agitation was stopped, and the emulsion was left to settle for 15 min to separate the oil and aqueous phase. The oil was removed, and the aqueous phase was transferred to a 50 mL-Falcon tube. Ethanol was added (ca. 30 mL) and the mixture was subsequently centrifuged at 3000 rpm and 30 °C for 10 min to eliminate the remaining oil. This washing step was repeated three times. The resulting alginate gel particles were left in ethanol until drying with scCO<sub>2</sub>.

#### 2.2.2. Preparation of alginate aerogel powder

The collected alginate aerogel particles were placed into paper cartridges and dried with scCO<sub>2</sub> as extraction medium (Waters-Thar Process, Pittsburg, PA, USA) at 40 °C, 120 bar and a CO<sub>2</sub> flow of 7 and 5 g/mL for 1 and 2.5 h, respectively (Fig. 1). The high-pressure vessel utilized had an internal volume of 100 mL (height: 4.2 cm; diameter: 5.5 cm). The depressurization rate was 1.0 g/min, and the depressurization duration was 66 min.

#### 2.2.3. BDP loading by scCO<sub>2</sub>-assisted impregnation

**2.2.3.1. Preparation of BDP-loaded alginate aerogels.** Alginate aerogels (200 mg) and BDP (20 or 40 mg) were filled separately in two filter paper cartridges and put at the bottom of the 100-mL stainless steel high-pressure vessel (Waters-Thar Process, Pittsburgh, PA, USA), ensuring

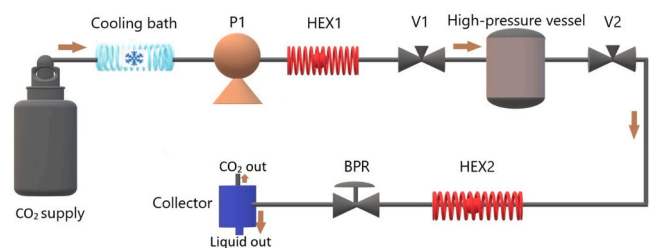


**Fig. 1.** Setup for continuous scCO<sub>2</sub> drying. P1: dual piston pump, V1-2: needle valves, HEX12: heat exchangers, BPR: backpressure regulator (used to maintain a stable pressure). Alginate algocol particles were placed in the high-pressure vessel. Residual ethanol was gathered via a collector.

that there was no physical contact between aerogels and the drug powder before the process. scCO<sub>2</sub>-assisted impregnation was carried out at 65 °C and 215 bar, based on previously reported solubility values [31]. Stirring was applied during the impregnation process (500 rpm). Besides varying the amount of initial BDP, different contact times (1, 2, 6, 9 and 24 h) and co-solvents (none, methanol, ethanol or acetone at 5 vol.%) were investigated. The depressurization step was controlled through an automatic backpressure (BPR in Fig. 1) at a flow of 1 g/min. Trials were carried out in triplicate.

**2.2.3.2. Quantification of BDP content in alginate aerogels.** Samples (ca. 10 mg) of the collected formulation were placed into vials containing 10 mL of a solvent mixture comprised of acetonitrile (ACN) and water at a 65:35 % v/v. Subsequently, the vials underwent sonication for 180 min to ensure the complete release of BDP present in the formulation into the solvent. BDP content in the aerogel particles was quantified by HPLC (JASCO, Tokyo, Japan) using a C18 column (Waters Symmetry 5 μm, 3.9 mm × 150 mm) as stationary phase. The mobile phase consisted of ACN:water at a 65:35 % v/v and was pumped at a flow rate of 1.4 mL/min. The volume of injection was 25 μL, and BDP was detected at 254 nm (retention time: 2.7 min). BDP concentration was calculated using a calibration curve with linearity in the 0.25–80 μg/mL concentration range (R<sup>2</sup> > 0.9999).

**2.2.3.3. Modelling of SCF impregnation of BDP into alginate aerogels.** The experimental data obtained from SCF-assisted impregnation were fitted to pseudo first-order and pseudo second-order kinetic models. By integrating Eq. 1, equations of pseudo first-order (Eq. 2) and pseudo second-order (Eq. 3) models were obtained:

$$\frac{d\left(1 - \frac{q_t}{q_c}\right)}{dt} = -k\left(1 - \frac{q_t}{q_c}\right)^n \quad (1)$$

$$\ln\left(\frac{q_c}{q_c - q_t}\right) = k_1 t \quad (2)$$

$$\frac{t}{q_t} = \frac{1}{k_2 q_c^2} + \frac{t}{q_c} \quad (3)$$

where  $q_t$  (mmol/g) represents the amount of drug that has been loaded into the aerogel after a specific contact time  $t$ ,  $q_c$  (mmol/g) denotes the adsorption capacity at equilibrium, which is the maximum quantity of drug that can be loaded into the aerogel, and  $k_1$  (1/h) and  $k_2$  (g/mmol·h) are the rate constants of pseudo first-order and pseudo second-order models, respectively. Fittings were carried out using OriginPro software (v. 9.0, Originlab, Northampton, MA, USA).

### 2.3. Physicochemical characterization

Alginate aerogel particle diameters were measured using a CKC53 optical microscope equipped with an EP50 camera and EPview image

analysis software (v.1.3, Olympus, Tokyo, Japan). The acquired images were subsequently analyzed using Fiji-ImageJ2 (National Institutes of Health, NIH, Bethesda, MD, USA) to determine the Feret diameter of the particles (Figure S1 in Supplementary Information).

Scanning electron microscopy (SEM, EVO LS15, Zeiss, Oberkochen, Germany) was used to study the morphology and structure of the aerogels. Sputter coating with a thin layer (2–20 nm) of iridium was employed to improve the contrast of the particles. The small grain size of iridium, typically between 1 and 2 nm, makes it a favorable coating material choice for capturing precise, high-magnification images [32].

Nitrogen adsorption-desorption analysis (ASAP2000, Micromeritics Inc., Norcross, GA, USA) was used to determine the specific surface area of BDP-loaded alginate aerogel particles. Before the analysis, samples were degassed under vacuum (< 1 mPa, room temperature, 24 h). The textural properties (specific surface area, pore size distribution and specific pore volume) were calculated using the BET and BJH methods.

The overall porosity ( $\epsilon$ ) of the material was calculated using (Eq. 4) [23]

$$\epsilon = \left(1 - \frac{\rho_{bulk}}{\rho_{skel}}\right) \times 100 \quad (4)$$

where  $\rho_{bulk}$  represents the bulk density and  $\rho_{skel}$  represents the skeletal density of the alginate particles. Bulk density was estimated based on the tapped density (approximately 1.26 times the tapped density according to existing literature) [23],[33]. The tapped density ( $\rho_{tapped}$ ) was calculated using the graduated flask method in triplicate [23]. Skeletal density was measured from five replicates using helium pycnometry (Quantachrome; Boynton Beach, FL, USA) at a temperature of 25 °C and a pressure of 1.03 bar.

The presence and potential interaction of BDP within the alginate aerogel was studied by Attenuated Total Reflectance (ATR) spectroscopy using a Varian FT-IR 670 spectrometer with a Gladi-ATR accessory (Pike Technologies, Madison, WI, USA). Pure BDP, alginate aerogels, BDP-loaded alginate aerogels and BDP-aerogel physical mixtures were examined in the 400–4000 cm<sup>-1</sup> range using 8 scans at a resolution of 2 cm<sup>-1</sup>.

X-ray diffraction (XRD) patterns were collected with a Rigaku MiniFlex diffractometer (Rigaku, Neu-Isenburg, Germany) operating at 30 kV and at 15 mA, with CuK<sub>α</sub> radiation (1.54056 Å) in the range from 3 to 60° (steps of 0.02°, scan step time of 2.00 s).

### 2.4. In vitro drug release

*In vitro* release tests of BDP-loaded alginate aerogels were carried out in dialysis bags (MWCO = 12,400 Da). Alginate aerogels (10 mg, containing ca. 450 μg of BDP) were added into the dialysis bags containing 1 mL of PBS solution, pH 7.4 (containing sodium chloride, potassium chloride, sodium phosphate and potassium phosphate) with 20 vol.% methanol to enhance the solubility of BDP (the solubility of BDP in PBS is 0.15 ± 0.04 μg/mL [34]). The entire setup was then placed in a plastic container containing 15 mL of the same medium and put inside a shaking incubator (100 rpm, 37 °C). Samples (300 μL) were periodically withdrawn for HPLC analysis, with an equivalent volume of fresh medium being reintroduced into the plastic container. Released BDP was quantified following the same HPLC method as described in Section 2.2.3.2.

Modeling of the BDP release profile from the aerogels was performed by fitting the data to the first-order release model (Eq. 5) and to two simultaneous first-order dissolution processes (Eq. 6 [35]) using GraphPad Prism 10 software (San Diego, CA, USA).

$$F = F_{max} (1 - e^{-k_1 t}) \quad (5)$$

$$D = D_{max,1} (1 - e^{-k_1 t}) + D_{max,2} (1 - e^{-k_2 t}) \quad (6)$$

Where  $D$  is the dosage of BDP released at time  $t$  (in percentage),  $D_{max,i}$  is

the maximum BDP released in stage  $i$  (in percentage), and  $k_i$  is the first-order kinetic coefficient in stage  $i$  in  $h^{-1}$ , being  $i=1$  or  $2$ .

### 2.5. *In vitro* aerosol deposition tests

Aerodynamic deposition of BDP-loaded alginate aerogels was evaluated with a Next Generation Impactor (NGI) manufactured by Copley (Nottingham, UK) consisting of seven stages and a Micro-Orifice Collector (MOC). A mouthpiece adapter was attached to the NGI to simulate the use of a single-dose DPI device with low resistance, meaning that through the device, the pressure drop is lower than  $5 \text{ Mbar}^{0.5} \text{ L/min}$ . The experimental setup involved a vacuum pump operating at a flow rate of  $100 \text{ L/min}$  for a duration of  $2.4 \text{ s}$ , resulting in a pressure drop of  $4 \text{ kPa}$  behind the impactor and an air volume of  $4 \text{ L}$ .

Inhaled particles in each stage articles were gathered using a solvent mixture of ACN:  $\text{H}_2\text{O}$   $65:35 \%$  v/v and subjected to  $180 \text{ min}$  of sonication. The quantity of BDP was then determined through HPLC analysis (cf. Section 2.2.3.2).

The mass of particles obtained at each stage was estimated from the drug measurements. With these results, the values of mass median aerodynamic diameter (MMAD), emitted fraction (EF), and fine particle fraction (FPF) were calculated [23],[36],[37]. The aerodynamic cut-off diameter of the NGI was set at  $6.12 \mu\text{m}$ ,  $3.42 \mu\text{m}$ ,  $2.18 \mu\text{m}$ ,  $1.31 \mu\text{m}$ ,  $0.72 \mu\text{m}$ ,  $0.14 \mu\text{m}$ , and  $0.24 \mu\text{m}$  for stages 1–7, correspondingly [38]. Emitted dose fraction (ED) was calculated as the percentage between the emitted dose ED (ED is the change in mass between the capsule before and after administration) and used total dose [36],[37]. The mass of particles with aerodynamic diameters  $<5 \mu\text{m}$  were marked as fine particle dose (FPD). Fine particle fraction (FPF) was expressed as the percentage of FPD versus ED. Mass median aerodynamic diameter (MMAD) was calculated based on the plotted graph of the cumulative mass percentage of the sample in probability scale versus the log of the stage cut-off diameter. All trials were conducted in triplicate ( $n = 3$ ) at room temperature.

### 2.6. *Ex vivo* bronchial permeability tests

Alginate aerogels ( $25 \text{ mg}$ ) loaded with BDP ( $6.0 \text{ wt.}\%$ ) were subjected to bronchial permeability experiments alongside an equivalent amount of drug powder ( $1.5 \text{ mg}$ ) for comparison. Freshly pig lungs (from a local slaughterhouse) were dissected, and the bronchial tissue was carefully cut, prepared, and washed with distilled water before being positioned in Franz cells for testing with the epithelial wall facing the donor chamber, and the basement membrane in contact with the receptor chamber to mimic biological conditions [39,40]. The stability of the tissue in the receptor medium was confirmed by observing that the tissue's color and texture remained unchanged after being placed in the medium for  $30 \text{ min}$  before commencing the permeability tests. The receptor chamber was filled with  $6 \text{ mL}$  of PBS:methanol ( $80:20 \text{ v/v}$ ), while the donor chamber contained  $500 \mu\text{L}$  of the same solvent mixture. The diffusion cells were kept at a constant temperature inside a methacrylate bath containing water with magnetic stirring ( $37 \text{ }^\circ\text{C}$ ,  $100 \text{ rpm}$ ). Aliquots of  $1 \text{ mL}$  were extracted from the receptor chamber hourly over a  $1$  and  $3$ -hour duration, and the withdrawn volume was replaced with fresh release medium. The aliquot samples underwent HPLC analysis as described in Section 2.2.3.2.

Following the permeability tests, the formulation remaining on the bronchial tissues after  $1$  and  $3 \text{ h}$  was carefully removed, and the bronchial tissues were washed in distilled water and stored at  $-80 \text{ }^\circ\text{C}$ . The bronchial tissues were later analyzed using IR-Raman spectroscopy (WITec, alpha 300 R, Wissenschaftliche Instrument und Technologie GmbH, Ulm, Germany) with a line scan in the  $xz$  plane and viewed through a  $50\times$  objective lens (Zeiss LD EC Epiplan-Neofluar Dic  $50\times/0.55$ ) (excitation wavelength:  $532 \text{ nm}$ , laser power:  $1.2 \text{ mW}$ , integration time:  $1.0 \text{ s}$ ). Each data point was gathered using  $100$  accumulations. IR-Raman spectroscopy is commonly employed for the detection of API within biological materials [41,42]. The study focused on the basement

membrane of bronchial tissue. The ratio between the BDP-associated peak at  $1666 \text{ cm}^{-1}$  and the fixed peak at  $1345 \text{ cm}^{-1}$  in lung tissue was compared to confirm the presence of BDP penetrated through bronchial tissue.

### 2.7. Statistical analysis

Results were presented as mean values and their corresponding standard deviations. One-way analysis of variance (ANOVA) followed by the post-hoc Tukey's Honestly Significant Difference (HSD) test was used to analyze the statistical significance. The groups exhibited a statistically significant difference when the  $p$ -value fell below  $0.05$ . All statistical analyses were conducted using GraphPad Prism 9 software (San Diego, CA, USA).

## 3. Results and discussion

### 3.1. Textural and physicochemical properties of alginate aerogels

A gelation-emulsification method was applied to produce alginate aerogel particles. This approach facilitates the upscaling of alginate particle production, transitioning from laboratory-scale to pilot and industrial scales, owing to its capacity to swiftly produce a stable emulsion with a consistent average droplet size within short times (typically minutes) [30]. Within this process, the precursor liquid formulation is transformed into spherical droplets within an immiscible liquid phase resulting in biphasic liquid-liquid system. Continuous stirring played a vital role as a constant energy source, aiding in the dispersion of the alginate aqueous solution into the oil phase to obtain a water-in-oil emulsion. Then,  $\text{CaCl}_2$  was introduced to the emulsion as a cross-linking agent to initiate gelation in the droplets of the dispersed phase of the emulsion resulting in a dispersion of alginate gel particles within the oil phase. Aerogel powder was obtained from the alginate gels dispersion after the removal of the oil and the extraction of the gel pore fluid by  $\text{scCO}_2$  drying.

The distinct characteristics of the alginate aerogels, including homogeneous particle size distribution, sphericity, high porosity and rough texture were observed by SEM imaging (Fig. 2(a-d)). These properties play a crucial role in facilitating the incorporation of poorly water-soluble drugs and make these particles promising candidates as carriers in novel DPI formulations [16]. Alginate aerogels had an average Feret diameter of  $2.25 \pm 1.50 \mu\text{m}$ , with an average circularity close to  $0.9$ . The size distribution of alginate aerogels was illustrated in Fig. 2e. Alginate aerogels possess a porous structure, which potentially mitigates difficulties regarding macrophage clearance and the movement of particles through the macrophage cytoskeleton when compared to rigid particles of the same size [43–45]. Certain studies emphasize the significance of stiffness in influencing how macrophages detect their presence within the lungs. In general, spherical particles lacking pores or exhibiting a rigid structure are more prone to uptake by macrophages than porous materials. Additionally, spherical particles, as well as other round-like shapes like pollen or cubic particles, tend to show better flow properties than other geometries (e.g., plate- and needle-shaped particles), which translates into a higher probability of deep lung deposition [15]. Using complementary analytical techniques (nitrogen adsorption-desorption analysis and helium pycnometry), the excellent textural properties of the aerogels were confirmed by a high porosity (*ca.*  $90\%$ ), high specific surface area ( $247 \pm 12 \text{ m}^2/\text{g}$ ), BJH-specific pore volume ( $0.8 \pm 0.04 \text{ cm}^3/\text{g}$ ) and average pore diameter within the mesoporous range ( $10.3 \pm 0.5 \text{ nm}$ ). In this context,  $\text{scCO}_2$  drying was very effective in preserving alginate aerogel textural properties with respect to other drying techniques for alginate particles [46].



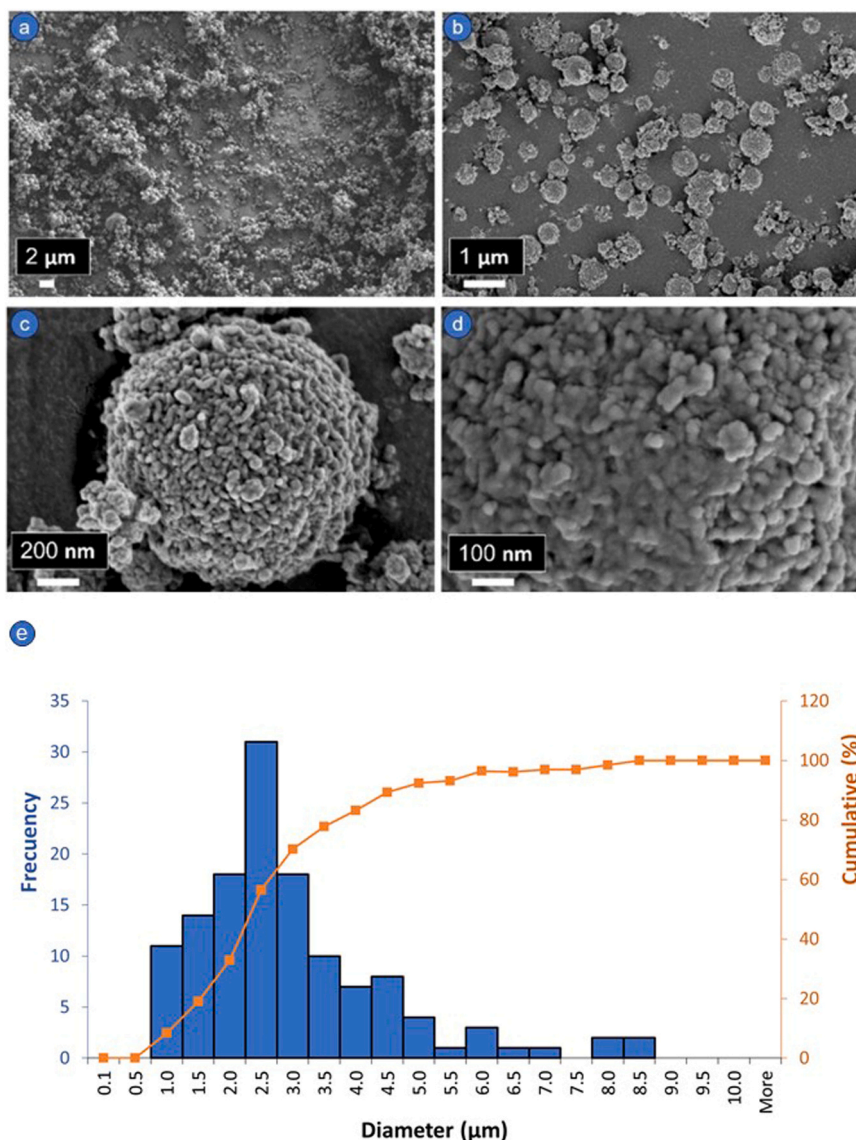


**Fig. 2.** Morphological appearance of the alginate aerogel particles obtained by gelation-emulsification evaluated by SEM imaging at different magnifications: (a,b) Narrow particle size distribution, (c) images of a representative spherical particle, (d) high mesoporosity and roughness on the surface and (e) size distribution of alginate aerogel carriers produced by gelation-emulsification technique followed by scCO<sub>2</sub> drying.

### 3.2. scCO<sub>2</sub> impregnation process for the incorporation of BDP into aerogels

#### 3.2.1. Effect of the processing parameters on BDP loading contents

BDP was loaded in the aerogels by a scCO<sub>2</sub> impregnation process where the temperature and pressure were set at 65 °C and 215 bar, respectively. The choice of these values was taken based on the stability for BDP reported within the 64.85–84.85 °C temperature range and the 213–385 bar pressure range [31]. Keeping these parameters fixed, the effects of the contact time (i.e., impregnation process duration at constant pressure and temperature), the initial amount of BDP loaded in the high-pressure vessel and the use of co-solvents on drug loading were studied.

Regarding contact time, the impregnation process was initially carried out using only scCO<sub>2</sub>. The duration of the impregnation process had a significant influence on the drug loadings (Fig. 3a). For short contact times (1 and 2 h), the drug loading was significantly lower compared to long impregnation periods of 6 and 9 h. However, much longer contact times (24 h) resulted in drug loading levels similar to those achieved at 9 h. The equilibrium state of the process seems to be achieved after 9 h,

although the BDP loadings in the aerogel were still low ( $0.19 \pm 0.02$  wt. %). The highly limited solubility of BDP in scCO<sub>2</sub> may explain this phenomenon as the highest solubility of BDP in scCO<sub>2</sub> measured by Vatanara et al. was  $3.36 \times 10^{-5}$  (mole fraction) at the harshest pressure (385 bar) and temperature (84.85 °C) conditions tested [31]. scCO<sub>2</sub> exhibits solvent characteristics that closely resemble those of traditional hydrocarbon solvents [26],[47]. scCO<sub>2</sub> is a good solvent for non-polar and low molecular weight solutes, but its solvation power is typically severely restricted when it comes to hydrophilic, polar molecules, or substances with a high molecular weight (>500 g/mol) [27],[47]. Although BDP is a hydrophobic molecule, BDP is also a large molecule that contains hydroxyl, carbonyl and ester functional groups within its structure, which are polar and could explain the limited solubility of the molecule in scCO<sub>2</sub> [48].

The effect of adding small amounts (5 vol.%) of different polar co-solvents (acetone, methanol and ethanol) on BDP loading was tested at short impregnation times (1 h). The addition of co-solvents significantly increased the BDP loading in the aerogel; the total amount loaded being dependent on the nature of the co-solvent (Fig. 3b). The scCO<sub>2</sub> solvent system affords an augmentation in polarity with the use of polar

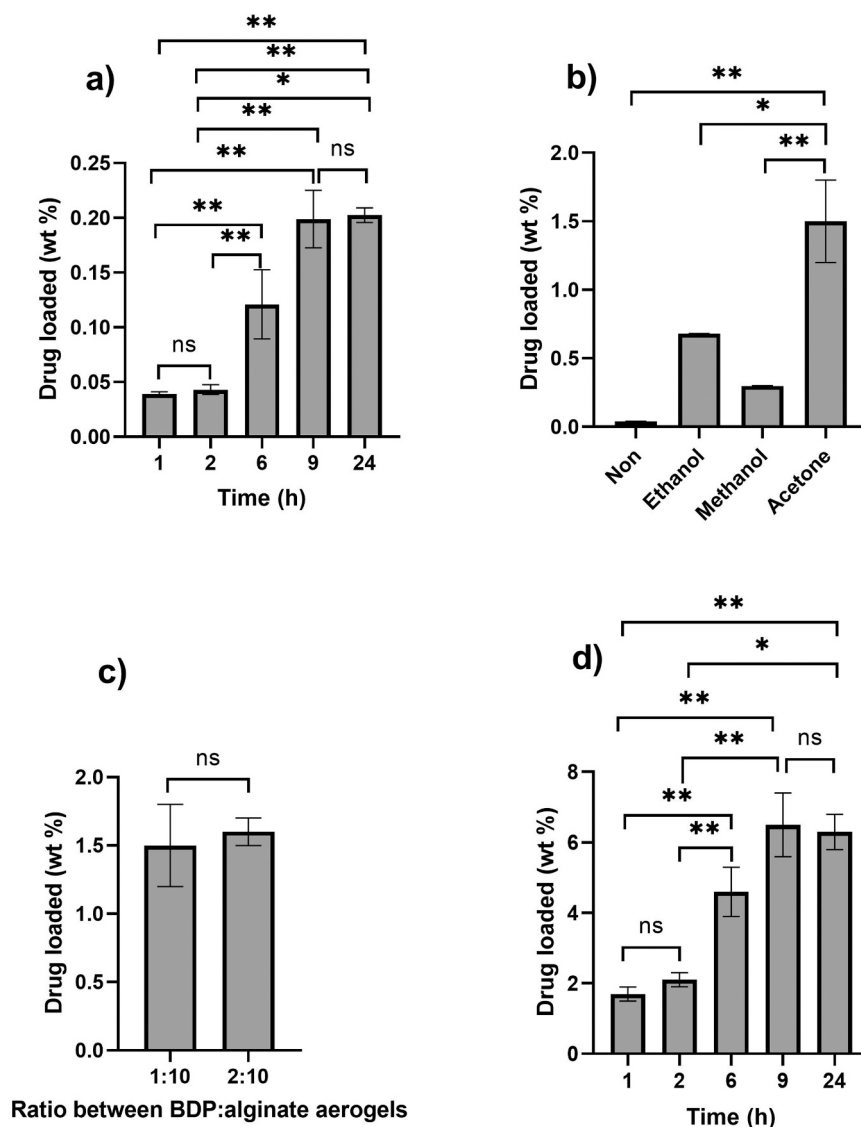


**Fig. 3.** Effect of processing parameters on the drug loading of BDP into alginate aerogels by scCO<sub>2</sub> impregnation: (a) Contact time using 1:10 BDP:aerogels weight ratio without co-solvent. (b) Addition of 5 vol.% of different co-solvents in a 1-hour impregnation process. (c) BDP:aerogel weight ratio with acetone as co-solvent. As a result, (d) increasing the contact time at the optimized conditions (5 vol.% acetone as co-solvent, 1:10 BDP:aerogels ratio) resulted in BDP-loadings > 6 wt%. (n = 3, mean ± standard deviation), \* and \*\* denote statistical differences (p < 0.05 and p < 0.01, respectively).

co-solvents, such as acetone and ethanol, at minor amounts resulting in a supercritical mixture with an effective increase in the solvation power of polar compounds [47]. This strategy not only broadens the range of compounds amenable to scCO<sub>2</sub> extraction and impregnation, but also showcases the versatility and adaptability of scCO<sub>2</sub> technologies in various applications, including pharmaceuticals, materials science and environmental chemistry [26],[47],[49].

BDP:aerogels weight ratio was increased from 1:10 to 1:5 in a scCO<sub>2</sub>/acetone impregnation medium to attempt to further increase the BDP-loading in the aerogels. However, doubling the amount of drug did not cause a significant change in drug loading (Fig. 3c). In the conducted experiment, the quantity of BDP was doubled while keeping constant other parameters, such as temperature, pressure, and depressurization rate. It is assumed that in both experimental cases, the transport to the aerogel pores' surface, the adsorption of the drug, and the precipitation of the drug remained unchanged [50]. The similar drug loading contents could be explained by the consistent dissolution of the drug in CO<sub>2</sub>/acetone supercritical medium, likely reaching the saturation in the said medium in both experimental cases regardless of the drug-to-aerogel carrier weight ratio used.

Acetone was the most effective co-solvent in increasing the BDP-loading in the aerogel particles by supercritical impregnation. The tests with this co-solvent at increasing contact times from 1 h to an extensive duration (24 h) were carried out to assess the maximum loadings of BDP with this supercritical mixture (Fig. 3d). The results followed a similar pattern to those obtained in pure scCO<sub>2</sub> but at much higher BDP loading values. During the initial stages of scCO<sub>2</sub> impregnation, the drug loading stood at ca. 2 wt%. However, a noteworthy increase in drug loading (ca. 5 wt.%) was observed at longer times of 6 h. The BDP loading significantly increased again after 9 h, achieving the highest drug loading capacity, which was not improved by extending the impregnation duration to 24 h. Overall, a moderately prolonged contact time coupled with the use of acetone as co-solvent emerges as a useful strategy for enhancing loading of BDP in aerogel systems by scCO<sub>2</sub> impregnation, and may be extended to enabling the efficient loading of other hydrophobic compounds.

### 3.2.2. Adsorption kinetics of BDP into alginate aerogels

The fitting of the experimental data from scCO<sub>2</sub> impregnation tests to kinetic models allows the prediction of the loading capacities that can be

achieved under certain given process conditions. The experimental BDP impregnation data from scCO<sub>2</sub> and CO<sub>2</sub>/acetone supercritical mixture obtained in this work (cf. Section 3.2.1) were fitted to the pseudo first-order and pseudo second-order models (Table 1, and Figure S2 in Supplementary Information). Pseudo first-order suggests that surface diffusion governs the rate-controlling step, while pseudo-second order indicates that the controlling factor is the chemical reaction [51].

Based on the calculated R<sup>2</sup> and Akaike information criterion AIC values (Table 1), the pseudo first-order kinetic model had a slightly higher R<sup>2</sup> and lower AIC indicating a higher level of accuracy in fitting the experimental data when compared to the pseudo second-order kinetic model, reflecting that the BDP adsorption rate-controlling step was the surface diffusion.

The maximum loading of BDP into alginate aerogels (q<sub>e</sub>) was 0.004 mmol/g in the case of scCO<sub>2</sub> impregnation, while it increased 28.5-fold with the use of acetone as co-solvent. According to the pseudo second-order model, ca. 75 wt.% of the maximum drug quantity was adsorbed within the initial 10 h in both experiments utilizing scCO<sub>2</sub>-assisted impregnation, with or without the presence of the co-solvent (acetone). Additionally, the kinetic coefficient k<sub>1</sub> in scCO<sub>2</sub>-assisted impregnation with co-solvent was higher than scCO<sub>2</sub>-assisted impregnation without co-solvent. This indicated an enhanced efficiency in the impregnation process when employing a co-solvent.

### 3.3. Physicochemical properties of BDP-loaded aerogels

The presence of BDP in the aerogels and its interaction with the alginate matrix was studied by ATR-FTIR (Fig. 4). BDP exhibited distinct conjugated and non-conjugated C=O stretching bands at 1724 cm<sup>-1</sup> and 1658 cm<sup>-1</sup>, respectively [36]. Characteristic C=C stretching band in BDP at 1615 cm<sup>-1</sup>, along with C-O bands at 1186 cm<sup>-1</sup> were also observed [10],[36]. ATR spectra of BDP-loaded alginate and physical mixture between BDP and alginate aerogels revealed a notable C=O stretching band at 1735 cm<sup>-1</sup> (asterisks in Fig. 4). This distinctive peak at 1735 cm<sup>-1</sup> suggested the presence of BDP in the loaded alginate aerogels.

The solid-state BDP in aerogel formulations containing BDP was investigated by XRD (Fig. 5). Crystalline BDP presents sharp and intense peaks at 11.28, 14.44, and 20.06° 2θ angles [10]. These peaks were clearly visible in the XRD pattern of a physical mixture of BDP and alginate aerogels, indicating that the simple mechanical mixing did not result in drug amorphization.

On the contrary, the pattern relevant to the impregnated aerogel indicated lack of crystalline drug being practically superimposable to that of the non-impregnated alginate aerogel. For a given drug:carrier matrix set, the selected temperature, pressure and depressurization steps are critical parameters of the scCO<sub>2</sub> impregnation process to achieve drug loadings in the amorphous form. The term "adsorptive precipitation" encompassed two essential phenomena that may take place during the scCO<sub>2</sub> impregnation process: the drug's adsorption onto the surface of polymers, and the drug's precipitation within the polymeric matrix. The high diffusivity and low surface tension of CO<sub>2</sub>, along with the presence of a co-solvent, played a significant role in dissolving the drug (BDP) in the supercritical fluid. Under controlled temperature and pressure conditions, scCO<sub>2</sub> underwent molecular density increase, followed by an expansion through the depressurization step, leading to the precipitation of drug molecules within the pore walls of the carrier

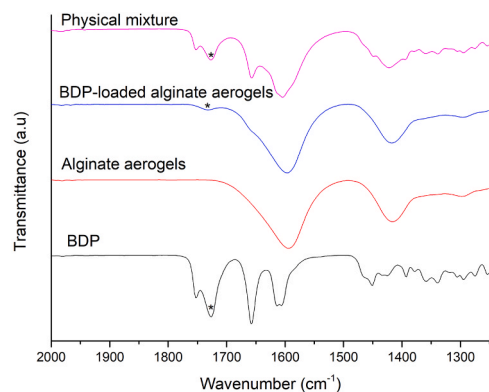


Fig. 4. ATR-FTIR spectra of the physical mixture of BDP and alginate compared to BDP-loaded alginate aerogel. Asterisks correspond to the wavenumber of 1735 cm<sup>-1</sup>, typical of C=O stretching band from BDP molecule. The physical mixture exhibits an equivalent BDP concentration in alginate aerogels, 6.5 wt.%.

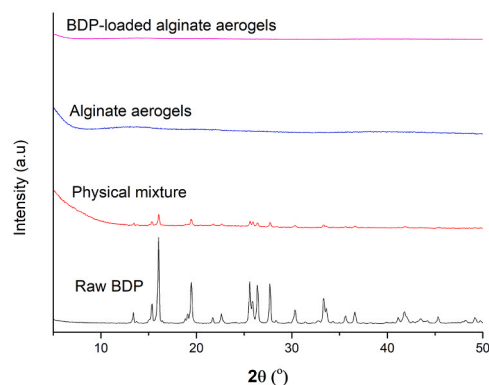


Fig. 5. X-ray diffraction patterns of alginate aerogels, BDP-loaded alginate aerogels, BDP and physical mixture of BDP and alginate aerogels. The physical mixture exhibits an equivalent BDP concentration in alginate aerogels, 6.5 wt.%.

material [50],[52]. In this context, the rapid precipitation or solidification of drug molecules caused the solid state of drug in an amorphous structure.

### 3.4. In vitro BDP release for aerogel carriers

BDP release from the aerogel matrix was examined via the dialysis bag method to avoid diffusion of the dissolving alginate chains to the receptor medium. The aerogels showed a two-phase release pattern, with an initial burst release in the first 15 min, followed by a sustained release over the next hours (Fig. 6). There was no significant difference in drug release between 3 and 7 h, suggesting that the drug release reached a plateau after 3 h.

The modelling of the BDP release profile from the aerogel unveiled a complex mechanistic behaviour (Table 2). The best fitting was obtained for the model considering a biexponential function (Eq. 6) where the

Table 1

Fitting parameters of the experimental data of BDP-loaded alginate aerogels obtained from scCO<sub>2</sub>-assisted impregnation with and without co-solvent (acetone) to the pseudo first-order (Eq. (2)) and pseudo second-order (Eq. (3)) adsorption kinetic models.

| Co-solvent used | Pseudo-first-order                        |                      |                |        | Pseudo-second-order                       |                           |                |        |
|-----------------|---|----------------------|----------------|--------|---|---------------------------|----------------|--------|
|                 | q <sub>e</sub> × 10 <sup>3</sup> (mmol/g) | k <sub>1</sub> (1/h) | R <sup>2</sup> | AIC    | q <sub>e</sub> × 10 <sup>3</sup> (mmol/g) | k <sub>2</sub> (g/mmol·h) | R <sup>2</sup> | AIC    |
| None            | 4.0±0.42                                  | 0.20±0.06            | 0.92           | -50.34 | 5.0±0.89                                  | 39.3±25.86                | 0.89           | -48.62 |
| Acetone         | 114±7.2                                   | 0.27±0.05            | 0.96           | -20.48 | 135±17.3                                  | 2.2±1.17                  | 0.89           | -16.35 |

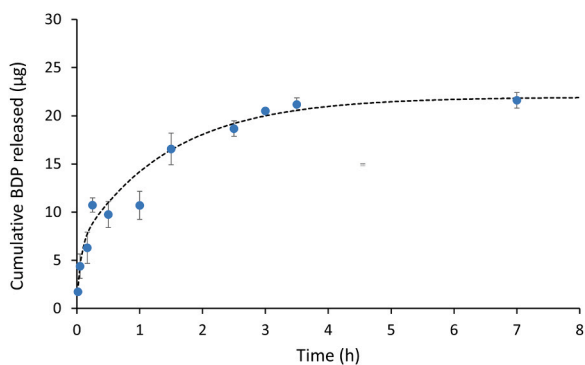


**Fig. 6.** *In vitro* release profile of BDP from alginate aerogels (PBS pH 7.4 with 20% methanol, 37 °C, 100 rpm) ( $n = 3$ , mean  $\pm$  standard deviation). Dashed line corresponds to the fitting of the data to the biexponential release model considering two simultaneous first-order dissolution processes (Eq. 6).

**Table 2**

Kinetic fitting parameters of the BDP release from alginate aerogel particles in PBS pH 7.4 with 20% methanol medium.

| Model              | First-order (Eq.5) | Double first-order (Eq.6) |
|--------------------|--------------------|---------------------------|
| $D_{\max,1}$ (%)   | $4.482 \pm 0.119$  | $1.43 \pm 0.19$           |
| $k_1$ ( $h^{-1}$ ) | $1.821 \pm 0.220$  | $17.00 \pm 5.69$          |
| $D_{\max,2}$ (%)   | -                  | $3.42 \pm 0.19$           |
| $k_2$ ( $h^{-1}$ ) | -                  | $0.692 \pm 0.101$         |
| $R^2$              | 0.938              | 0.979                     |

mass transfer mechanism is mainly governed by dissolution [35],[53]. This model considers two simultaneous first-order drug releases of two different BDP fractions. A first BDP fraction ( $k_1$ ,  $D_{\max,1}$ ) weakly bound to the surface of alginate of the aerogel matrix with a fast dissolution and diffusion to the release medium. A second BDP fraction ( $k_2$ ,  $D_{\max,2}$ ) with

a complex interaction with the aerogel and transport through the nanoporous matrix that includes the hydration of the aerogels, PBS diffusion through the pores towards the interior part of the particles, and a combined mechanism of dissolution of BDP at the surface inside the pores and disassembly of the alginate chains due to ion exchange. The amount of drug released under the second effect accounted for a significant portion, specifically 70% of the overall drug released, amounting to an equivalent of 15  $\mu$ g.

Together with the lipophilic nature of BDP ( $\log P=3.49$ ), the physiological characteristics of human lung conditions, such as the presence of surfactants and the lipophilic nature of the epithelia, did not perfectly mirror the conditions observed in the *in vitro* release with an aqueous release medium [14],[54]. Consequently, this difference accounted for the low amount of BDP released from alginate aerogels (ca. 22  $\mu$ g, equivalent to ca. 4.5 wt.% after 6 h). In another work, the drug release study utilized a commercial product of BDP (Clenil®) as a control [9]. Vertical Franz diffusion cells were employed in DPBS with artificial mucus. Following a 6-hour incubation period, the BDP released from the Clenil® formulation was close to 1.5 wt.%, indicating a very low release rate, even though artificial mucus was used to mimic the lung conditions.

### 3.5. *In vitro* aerodynamic drug deposition of BDP-loaded alginate aerogels

BDP-loaded aerogel formulations obtained from scCO<sub>2</sub> impregnation at different durations (1, 6, 9 and 24 h) with 5 vol.% acetone (1:10 BDP:aerogels weight ratio) were subjected to aerosol performance testing using an NGI impactor (Fig. 7 and Table 3). This enabled the precise measurement and characterization of the amount of BDP deposited at each stage of the NGI, providing valuable insights into the aerodynamic deposition behavior of the aerogels. In general, similar drug deposition profiles were observed regardless of the scCO<sub>2</sub> impregnation time, with only changes in the total amount of drug

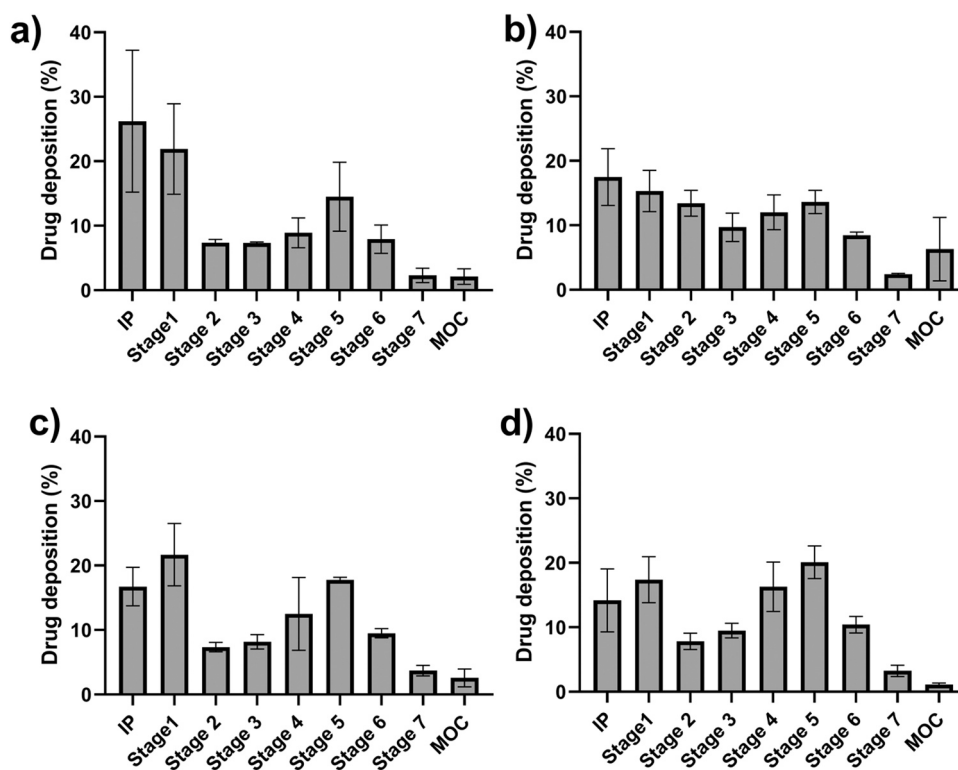


**Fig. 7.** Drug deposition of BDP-loaded alginate aerogels obtained from scCO<sub>2</sub> impregnation with different contact times: (a) 1 h, (b) 6 h, (c) 9 h and (d) 24 h ( $n = 3$ , mean  $\pm$  standard deviation). Notation: IP, induction port, and MOC, micro-orifice collector.



**Table 3**

*In vitro* aerodynamic properties obtained from the *in vitro* deposition tests for the BDP-loaded alginate aerogels prepared by scCO<sub>2</sub> impregnation using acetone as co-solvent at different contact times.

| Impregnation time (h) | MMAD ( $\mu\text{m}$ ) | EF (%)         | FPF (%)      |
|-----------------------|------------------------|----------------|--------------|
| 1                     | 1.2 $\pm$ 0.2          | 86.8 $\pm$ 5.4 | 78 $\pm$ 3.5 |
| 6                     | 1.1 $\pm$ 0.1          | 89.6 $\pm$ 1.0 | 80 $\pm$ 1.7 |
| 9                     | 1.1 $\pm$ 0.1          | 89.6 $\pm$ 1.1 | 80 $\pm$ 1.6 |
| 24                    | 1.1 $\pm$ 0.1          | 87.3 $\pm$ 2.9 | 80 $\pm$ 3.5 |

deposited due to the different loading contents.

A wide range of important parameters can be assessed when evaluating drug aerodynamics *in vitro*, including mass median aerodynamic diameter (MMAD), emitted fraction (EF), and fine particle fraction (FPF) [23]. MMAD refers to the aerodynamic diameter at which 50 % of the total particle mass exhibits a diameter smaller than the median, while the other 50 % exhibits a diameter larger than the median. In the case of the BDP-loaded alginate aerogels, the mean value (ca. 1.1  $\mu\text{m}$ ) indicated that particles were within the 1–5  $\mu\text{m}$  range with a propensity to settle predominantly in the bronchioles and alveoli, which constitute the target region for efficient drug delivery. EF quantifies the percentage of drug recovered in the NGI, representing the overall dose emitted during the evaluation. The remarkable EF (ca. 90 %) of the aerogel particles indicated the high flowability of the inhaled formulation leading to a high amount of drug entering to the NGI and to a small residual amount remaining in the capsule. The high flowability of inhaled formulation also confirmed the successful removal of the acetone after impregnation. A significant portion (ca. 20 %) of the BDP content in the loaded aerogel particles was primarily deposited in the throat and initial stages. However, towards the final stages, the drug content approached to low levels, endorsing that a substantial amount of BDP would not be exhaled again and could be effectively delivered to the bronchioles and bronchi within the respiratory system for a local treatment. Lastly, FPF measured the fraction of the emitted dose that consisted of particles with an aerodynamic size below 5  $\mu\text{m}$ . The high FPF value of the alginate aerogels (ca. 80 %) indicated their suitability for localized treatment, as it facilitates targeted drug delivery to the specific regions of interest. The findings suggested superior performance of inhaled particles utilizing alginate aerogels in comparison to commercial products containing BDP, like Foster® NEXThaler®, which exhibited an FPF of less than 70 % [55], [56]. Overall, the similar *in vitro* aerodynamic properties of inhaled formulations obtained from different impregnation contact times indicated that the contact time in scCO<sub>2</sub> impregnation process did not cause detrimental effects on the aerodynamic performance of the formulation containing BDP.

### 3.6. *Ex vivo* permeability studies

Once the capability of the aerogels to access to lung tissue was demonstrated, *ex vivo* permeability analysis was carried out using porcine bronchial tissue to measure the capacity of the drug to be released from the carrier and its penetration into the bronchial tissue (Fig. 8). Porcine lungs were used in this study due to their similarity with human lungs in terms of size and anatomical features [57]. Additionally, porcine lungs exhibit comparable IgE levels, smooth muscle structure, and effective trypsinase inhibitors, which are crucial factors in the study of respiratory allergies and asthma.

According to the findings in Fig. 8a, the presence of BDP in the receptor chamber indicated that BDP was not only released from the inhaled formulation but also permeated through the bronchial tissue. There was no statistically significant difference between the amount of BDP permeated between 1 and 2 h in the receptor chamber. The maximum amount of BDP permeated at the *ex vivo* experiment was ca. 4  $\mu\text{g}/\text{cm}^2$  with the available permeation area in the Franz cells being 0.785  $\text{cm}^2$ , which corresponded to 3.2  $\mu\text{g}$  of BDP and 0.4 wt.% of total

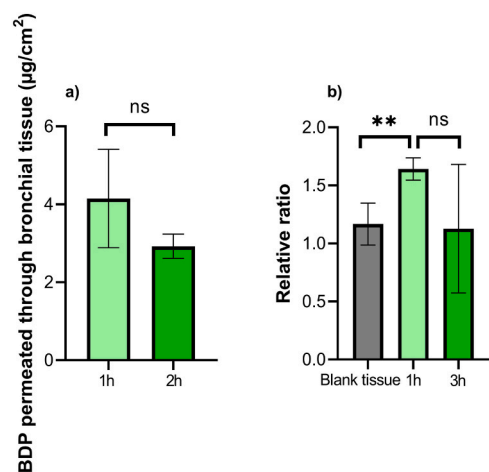


**Fig. 8.** *Ex vivo* BDP permeation studies of drug-loaded aerogel particles: (a) Cumulative quantities of BDP that permeated across porcine bronchial tissue after 1 and 2 h (n = 3; mean values  $\pm$  standard deviations). (b) Ratio of Raman peak intensities of BDP in the basement membrane of the tissue, that indicated the presence of BDP. Gray color was employed to represent blank tissues, light green and dark green was employed to represent tissues containing inhaled formulation after 1 and 3 h contact, respectively.

BDP amount. This BDP amount represents only the drug that passed through the tissues and entered to the receptor chamber, but the total BDP released include what remained in the donor chamber and what was retained within the tissue.

The measured BDP amount in the *ex vivo* test was notably lower than the *in vitro* release (22  $\mu\text{g}$ ). This difference was related to the smaller volume of the release medium in the receptor chamber in Franz cells of the *ex vivo* test and the reduced permeation area of the tissue in comparison to the dialysis bag. Moreover, the drug permeation surface area of the dialysis bags and of the Franz cells are 32  $\text{cm}^2$  and 0.785  $\text{cm}^2$ , respectively, which are much lower than the total airway surface area in human lungs, spanning from the trachea to the bronchioles and alveoli, with values of approximately 0.24  $\text{m}^2$  and 70  $\text{m}^2$ , respectively [58,59]. Higher total drug amounts would be absorbed under the available surface area in real body conditions to reach therapeutic doses.

After 3 h, the quantification of BDP through the HPLC method was not feasible, probably due to: (1) the dilution effect in the receptor chamber after sampling and replenishment with fresh medium, (2) the incomplete release of BDP from their carriers and limited solubility of BDP in the release medium of PBS:methanol 80:20 v/v, (3) the accumulation of BDP inside the tissues or (4) the instability of BDP inside the bronchial tissue after 2 h. Due to the presence of esterases in the lung, the hydrolysis of BDP produces three distinct metabolites: the active compound beclomethasone-17-monopropionate (BMP) and two inactive compounds with low binding affinity to the glucocorticoid receptor: beclomethasone-21-monopropionate (21-BMP), and beclomethasone (BOH) [11,56]. BDP was reported to be transformed into inactive metabolites upon incubation with lung tissue, with BMP being the predominant (after 2 and 6 h), while BOH was the primary metabolite (after 24 h).

The presence of BDP in the bronchial tissue was verified through IR-Raman spectroscopy (Fig. 8b). A comparison was made between the bronchial tissue after 1 and 3 h of incubation in the Franz cell containing the inhaled formulation in contrast to the control bronchial tissue. After 1 h, the relative ratio obtained from BDP-loaded alginate aerogels of the basement membrane of the bronchial tissue was higher compared to the non-treated bronchial tissue. These findings suggested that BDP contained in the inhaled formulation was released from the alginate carriers and successfully penetrated the bronchial tissue after 1 h. There was no statistically significant difference between the signals recorded for

bronchial tissues that were 1 h or 3 h in contact with the BDP-loaded alginate aerogels. The observed outcome can be attributed to certain limitations inherent in this experiment that were highlighted above.

In general, the findings from the *ex vivo* permeability tests employing porcine bronchial tissue demonstrated the potential of BDP-loaded alginate aerogels to be released from the aerogels and to penetrate into the porcine bronchial tissue. Several strategies can be implemented to enhance drug release or permeation for these studies: (1) augmenting the volume of the medium to achieve sink conditions, (2) increasing the available surface area for drug release or permeation, or (3) adjusting the hydration of alginate aerogels. BDP in the inhaled formulation deposited on the surface and within alginate aerogel pores. Upon contact with the medium, BDP initially dissolved, and later, the medium interacted with the aerogels, releasing BDP from pores [52]. However, when pores contacted the solvent, alginate aerogels' hydration might cause structural collapse and swelling, potentially entrapping BDP. Hence, further experiments on modifying the hydration and its correlation with drug release and permeation profiles could enhance the release behavior of the inhaled formulation.

#### 4. Conclusions

The combination of the gelation-emulsification method and the scCO<sub>2</sub> technological platform allows to produce alginate aerogels with great potential for pulmonary delivery of BDP by using green and environmentally friendly processes. The parameters of co-solvent selection for the impregnation process and contact time highly influenced the drug loading capacity. Namely, optimal conditions of 9 hours of contact time and use of 5 vol.% of acetone resulted in a 28.5-fold increase in BDP loading compared to scCO<sub>2</sub> impregnation performed without co-solvents. The kinetics of supercritical impregnation could be fitted to a pseudo first-order model to gain insight into the adsorption process. The *in vitro* release behavior of BDP-loaded alginate aerogels exhibited an initial rapid release (1.4 wt.% of total amount of BDP contained in alginate aerogels) followed by a sustained release (3.4 wt.% of total amount of BDP contained in alginate aerogels), which was fitted by a biexponential function. The aerogels had excellent flowability and desirable aerodynamic sizes ranging around 1 μm as indicated in the deposition tests, suggesting for deep lung deposition. The presence of BDP in the porcine lung tissues indicated that BDP could be released from alginate aerogels and penetrate the bronchial porcine lung tissues. Overall, the application of green technology utilizing scCO<sub>2</sub>, as implemented here, shows significant potential for producing inhaled formulations featuring a low excipient-to-drug ratio (10:1), in contrast to commercial products characterized by a higher ratio (100:1). This provides advantages in terms of increased convenience and comfort for inhaler usage, particularly for individuals who rely on inhalers on a daily basis.

#### CRedit authorship contribution statement

**Inés Ardao:** Writing – review & editing, Data curation. **Ruggero Bettini:** Writing – review & editing, Supervision, Methodology. **Carmen Alvarez-Lorenzo:** Writing – review & editing, Supervision, Methodology. **Carlos A Garcia-Gonzalez:** Writing – review & editing, Writing – original draft, Supervision, Resources, Project administration, Methodology, Investigation, Funding acquisition. **Thoa Duong:** Writing – review & editing, Writing – original draft, Methodology, Investigation. **Clara López-Iglesias:** Writing – review & editing. **Annalisa Bianchera:** Writing – review & editing, Supervision, Methodology. **María Vivero-López:** Methodology, Investigation.

#### Declaration of Competing Interest

Authors declare no competing interests

#### Data Availability

Data will be made available on request.

#### Acknowledgments

Work supported by MICINN [PID2020–120010RB-I00/AEI/10.13039/501100011033], Agencia Estatal de Investigación [AEI] and FEDER funds. This publication is based upon work from ECO-AEROGELS COST Innovation Grant (ref. IG18125) supported by the European Commission. Th. D. acknowledges the support of Diputación Provincial de A Coruña for research in health science 2022–2023 (BINV-CS/2022) and of AEROGELS COST Action (ref. CA18125) for a Short Term Scientific Missions (STSM) grant to undergo the *in vitro* aerodynamic drug deposition tests of aerogels in the University of Parma (Italy). Clara López-Iglesias acknowledges Xunta de Galicia for her Postdoctoral contract (ED481B 2021/008). The authors would like to thank Ezequiel Vázquez Fernández, Carlos Illanes-Bordomás and Miguel Pereira-Silva (University of Santiago de Compostela, Spain) for their valuable support and technical help with Raman spectroscopy, analysis of SEM images and dialysis method in *in vitro* drug release studies, respectively.

#### Appendix A. Supporting information

Supplementary data associated with this article can be found in the online version at [doi:10.1016/j.jcou.2024.102722](https://doi.org/10.1016/j.jcou.2024.102722).

#### References

- [1] H.-Y. Li, Alginate-Based Inhalable Particles for Controlled Pulmonary Drug Delivery, in: S. Jana, S. Jana (Eds.), *Alginate Biomaterial*, Springer Nature Singapore, Singapore, 2023, pp. 207–240, [https://doi.org/10.1007/978-981-19-6937-9\\_9](https://doi.org/10.1007/978-981-19-6937-9_9).
- [2] H.I. Shahin, L. Chablani, A comprehensive overview of dry powder inhalers for pulmonary drug delivery: challenges, advances, optimization techniques, and applications, *J. Drug Deliv. Sci. Technol.* 84 (2023) 104553, <https://doi.org/10.1016/j.jddst.2023.104553>.
- [3] K. Kadota, T.R. Sosnowski, S. Tobita, I. Tachibana, J.Y. Tse, H. Uchiyama, Y. Tozuka, A particle technology approach toward designing dry-powder inhaler formulations for personalized medicine in respiratory diseases, *Adv. Powder Technol.* 31 (2020) 219–226, <https://doi.org/10.1016/j.apt.2019.10.013>.
- [4] A. Ari, B.R. Alhamad, Evaluating dry powder inhalers: from in vitro studies to mobile health technologies, *Respir. Med.* 215 (2023) 107281, <https://doi.org/10.1016/j.rmed.2023.107281>.
- [5] R. Scherließ, S. Bock, N. Bungert, A. Neustock, L. Valentin, Particle engineering in dry powders for inhalation, *Eur. J. Pharm. Sci.* 172 (2022) 106158, <https://doi.org/10.1016/j.ejps.2022.106158>.
- [6] A.M. Healy, M.I. Amaro, K.J. Paluch, L. Tajber, Dry powders for oral inhalation free of lactose carrier particles, *Adv. Drug Deliv. Rev.* 75 (2014) 32–52, <https://doi.org/10.1016/j.addr.2014.04.005>.
- [7] P. Party, R. Ambrus, Investigation of physico-chemical stability and aerodynamic properties of novel “nano-in-micro” structured dry powder inhaler system, *Micromachines* 14 (2023) 1348, <https://doi.org/10.3390/mi14071348>.
- [8] Z. Huang, L. Lin, C. McGoverin, H. Liu, L. Wang, Q. (Tony) Zhou, M. Lu, C. Wu, Dry powder inhaler formulations of poorly water-soluble itraconazole: a balance between in-vitro dissolution and in-vivo distribution is necessary, *Int. J. Pharm.* 551 (2018) 103–110, <https://doi.org/10.1016/j.ijpharm.2018.09.018>.
- [9] E.F. Craparo, S.E. Drago, G. Costabile, M. Ferraro, E. Pace, R. Scaffaro, F. Ungaro, G. Cavallaro, Sustained-release powders based on polymer particles for pulmonary delivery of beclomethasone dipropionate in the treatment of lung inflammation, *Pharmaceutics* 15 (2023) 1248, <https://doi.org/10.3390/pharmaceutics15041248>.
- [10] L. Casula, F. Lai, E. Pini, D. Valenti, C. Sinico, M.C. Cardia, S. Marceddu, G. Ailuno, A.M. Fadda, Pulmonary delivery of curcumin and beclomethasone dipropionate in a multicomponent nanosuspension for the treatment of bronchial asthma, *Pharmaceutics* 13 (2021) 1300, <https://doi.org/10.3390/pharmaceutics13081300>.
- [11] M.G. Matera, B. Rinaldi, L. Calzetta, P. Rogliani, M. Cazzola, Pharmacokinetics and pharmacodynamics of inhaled corticosteroids for asthma treatment, *Pulm. Pharmacol. Ther.* 58 (2019) 101828, <https://doi.org/10.1016/j.pupt.2019.101828>.
- [12] Easyhaler Beclometasone 200micrograms/dose dry powder inhaler (Orion Pharma (UK) Ltd) 200 dose - RightBreathe, (n.d.). (<https://www.rightbreathe.com/medicines/easyhaler-beclometasone-200microgramsdose-dry-powder-inhaler-orion-pharma-uk-ltd-200-dose/>) (accessed November 6, 2023).

- [13] Fostair NEXThaler 200 micrograms/6 micrograms per actuation inhalation powder - Summary of Product Characteristics (SmPC) - (emc), (n.d.). (<https://www.medicines.org.uk/emc/product/5075/smpc#ref>) (accessed January 25, 2023).
- [14] J.E. Hastedt, P. Bäckman, A.R. Clark, W. Doub, A. Hickey, G. Hochhaus, P.J. Kuehl, C.-M. Lehr, P. Mauser, J. McConville, R. Niven, M. Sakagimi, J.G. Weers, Scope and relevance of a pulmonary biopharmaceutical classification system AAPS/FDA/USP Workshop March 16-17th, 2015 in Baltimore, MD, AAPS Open 2 (2016) 1, <https://doi.org/10.1186/s41120-015-0002-x>.
- [15] T. Duong, C. López-Iglesias, P.K. Szewczyk, U. Stachewicz, J. Barros, C. Alvarez-Lorenzo, M. Alnaief, C.A. García-González, A pathway from porous particle technology toward tailoring aerogels for pulmonary drug administration, *Front. Bioeng. Biotechnol.* 9 (2021) 671381, <https://doi.org/10.3389/fbioe.2021.671381>.
- [16] P. Chakravarty, A. Famili, K. Nagapudi, M.A. Al-Sayah, Using supercritical fluid technology as a green alternative during the preparation of drug delivery systems, *Pharmaceutics* 11 (2019) 629, <https://doi.org/10.3390/pharmaceutics11120629>.
- [17] G.D. Hadiwinoto, P.C. Lip Kwok, R. Lakerveld, A review on recent technologies for the manufacture of pulmonary drugs, *Ther. Deliv.* 9 (2018) 47–70, <https://doi.org/10.4155/tde-2017-0083>.
- [18] L. Goimil, M.E.M. Braga, A.M.A. Dias, J.L. Gómez-Amoza, A. Concheiro, C. Alvarez-Lorenzo, H.C. de Sousa, C.A. García-González, Supercritical processing of starch aerogels and aerogel-loaded poly( $\epsilon$ -caprolactone) scaffolds for sustained release of ketoprofen for bone regeneration, *J. CO2 Util.* 18 (2017) 237–249, <https://doi.org/10.1016/j.jcou.2017.01.028>.
- [19] D. Lovskaya, N. Menshutina, Alginate-based aerogel particles as drug delivery systems: investigation of the supercritical adsorption and in vitro evaluations, *Materials* 13 (2020) 329, <https://doi.org/10.3390/ma13020329>.
- [20] C.A. García-González, T. Budtova, L. Durães, C. Erkey, P. Del Gaudio, P. Gurikov, M. Koebel, F. Liebner, M. Neagu, I. Smirnova, An Opinion Paper on Aerogels for Biomedical and Environmental Applications, *Molecules* 24 (2019) 1815, <https://doi.org/10.3390/molecules24091815>.
- [21] M. Guastaferrero, E. Reverchon, L. Baldino, Polysaccharide-based aerogel production for biomedical applications: a comparative review, *Materials* 14 (2021) 1631, <https://doi.org/10.3390/ma14071631>.
- [22] S. Karamikamkar, E.P. Yalcintas, R. Haghniaz, N.R. de Barros, M. Mecwan, R. Nasiri, E. Davoodi, F. Nasrollahi, A. Erdem, H. Kang, J. Lee, Y. Zhu, S. Ahadian, V. Jucaud, H. Maleki, M.R. Dokmeci, H. Kim, A. Khademhosseini, Aerogel-based biomaterials for biomedical applications: from fabrication methods to disease-targeting applications, *Adv. Sci.* (2023) 2204681, <https://doi.org/10.1002/adv.202204681>.
- [23] C. López-Iglesias, A.M. Casielles, A. Altay, R. Bettini, C. Alvarez-Lorenzo, C. A. García-González, From the printer to the lungs: inkjet-printed aerogel particles for pulmonary delivery, *Chem. Eng. J.* 357 (2019) 559–566, <https://doi.org/10.1016/j.cej.2018.09.159>.
- [24] M. Alnaief, R.M. Obaidat, M.M. Alsmadi, Preparation of hybrid alginate-chitosan aerogel as potential carriers for pulmonary drug delivery, *Polymers* 12 (2020) 2223, <https://doi.org/10.3390/polym12102223>.
- [25] T. Athamneh, A. Amin, E. Benke, R. Ambrus, P. Gurikov, I. Smirnova, C.S. Leopold, Pulmonary drug delivery with aerogels: engineering of alginate and alginate-hyaluronic acid microspheres, *Pharm. Dev. Technol.* 26 (2021) 509–521, <https://doi.org/10.1080/10837450.2021.1888979>.
- [26] M. Tadesse Abate, A. Ferri, J. Guan, G. Chen, V. Nierstrasz, Impregnation of Materials in Supercritical CO<sub>2</sub> to Impart Various Functionalities, in: I. Piro (Ed.), *Advanced Supercritical Fluids Technologies*, IntechOpen, 2020, <https://doi.org/10.5772/intechopen.89223>.
- [27] M. Champeau, J.-M. Thomassin, T. Tassaing, C. Jérôme, Drug loading of polymer implants by supercritical CO<sub>2</sub> assisted impregnation: a review, *J. Control. Release* 209 (2015) 248–259, <https://doi.org/10.1016/j.jconrel.2015.05.002>.
- [28] R.K. Kankala, Y.S. Zhang, S. Wang, C. Lee, A. Chen, Supercritical fluid technology: an emphasis on drug delivery and related biomedical applications, *Adv. Healthc. Mater.* 6 (2017) 1700433, <https://doi.org/10.1002/adhm.201700433>.
- [29] J.F.A. Valente, J.R. Dias, A. Sousa, N. Alves, Composite central face design—An approach to achieve efficient alginate microcarriers, *Polymers* 11 (2019) 1949, <https://doi.org/10.3390/polym11121949>.
- [30] K. Ganesan, T. Budtova, L. Ratke, P. Gurikov, V. Baudron, I. Preibisch, P. Niemeyer, I. Smirnova, B. Milow, Review on the production of polysaccharide aerogel particles, *Materials* 11 (2018) 2144, <https://doi.org/10.3390/ma11112144>.
- [31] A. Vatanara, A. Najafabadi, M. Khajeh, Y. Yamini, Solubility of some inhaled glucocorticoids in supercritical carbon dioxide, *J. Supercrit. Fluids* 33 (2005) 21–25, [https://doi.org/10.1016/S0896-8446\(04\)00112-3](https://doi.org/10.1016/S0896-8446(04)00112-3).
- [32] R. Heu, S. Shahbazmohamadi, J. Yorston, P. Capeder, Target material selection for sputter coating of SEM samples, *Micros. Today* 27 (2019) 32–36, <https://doi.org/10.1017/S1551929519000610>.
- [33] D. Wu, C. Wang, J. Yang, H. Wang, H. Han, A. Zhang, Y. Yang, Q. Li, Improving the intracellular drug concentration in lung cancer treatment through the codelivery of doxorubicin and miR-519c mediated by porous PLGA microparticle, *Mol. Pharm.* 13 (2016) 3925–3933, <https://doi.org/10.1021/acs.molpharmaceut.6b00702>.
- [34] I. Khan, S. Yousaf, M. Najlah, W. Ahmed, A. Elhissi, Proliposome powder or tablets for generating inhalable liposomes using a medical nebulizer, *J. Pharm. Investig.* 51 (2021) 61–73, <https://doi.org/10.1007/s40005-020-00495-8>.
- [35] C.A. García-González, J. Barros, A. Rey-Rico, P. Redondo, J.L. Gómez-Amoza, A. Concheiro, C. Alvarez-Lorenzo, F.J. Monteiro, antimicrobial properties and osteogenicity of vancomycin-loaded synthetic scaffolds obtained by supercritical foaming, *ACS Appl. Mater. Interfaces* 10 (2018) 3349–3360, <https://doi.org/10.1021/acsami.7b17375>.
- [36] H.-T. Wu, H.-C. Lin, Y.-J. Tu, K.H. Ng, Instant formulation of inhalable beclomethasone dipropionate—gamma-cyclodextrin composite particles produced using supercritical assisted atomization, *Pharmaceutics* 15 (2023) 1741, <https://doi.org/10.3390/pharmaceutics15061741>.
- [37] N. Nimmano, S.B.M. Mohari, Comparison of efficacies of full and abbreviated cascade impactors in aerosol characterization of nebulized salbutamol sulfate produced by a jet nebulizer, *PHAR* 68 (2021) 899–905, <https://doi.org/10.3897/pharmacia.68.e76072>.
- [38] V.A. Marple, D.L. Roberts, F.J. Romay, N.C. Miller, K.G. Truman, M. Van Oort, B. Olsson, M.J. Holroyd, J.P. Mitchell, D. Hochrainer, Next generation pharmaceutical impactor (a new impactor for pharmaceutical inhaler testing). part i: design, *J. Aerosol Med.* 16 (2003) 283–299, <https://doi.org/10.1089/089426803769017659>.
- [39] J. Nesamony, A. Kalra, M.S. Majrad, S.H.S. Boddu, R. Jung, F.E. Williams, A. M. Schnapp, S.M. Nauli, A.L. Kalinoski, Development and characterization of nanostructured mists with potential for actively targeting poorly water-soluble compounds into the lungs, *Pharm. Res.* 30 (2013) 2625–2639, <https://doi.org/10.1007/s11095-013-1088-2>.
- [40] T. Duong, M. Vivero-Lopez, I. Ardao, C. Alvarez-Lorenzo, A. Forgács, J. Kalmár, C. A. García-González, Alginate aerogels by spray gelation for enhanced pulmonary delivery and solubilization of beclomethasone dipropionate, *Chem. Eng. J.* 485 (2024) 149849, <https://doi.org/10.1016/j.cej.2024.149849>.
- [41] A. Kattar, A. Quelle-Regaldie, L. Sánchez, A. Concheiro, C. Alvarez-Lorenzo, Formulation and characterization of epalrestat-loaded polysorbate 60 cationic liposomes for ocular delivery, *Pharmaceutics* 15 (2023) 1247, <https://doi.org/10.3390/pharmaceutics15041247>.
- [42] E. Pena-Rodríguez, T. García-Berrococo, E. Vázquez Fernández, F.J. Otero-Espinar, J. Abian, F. Fernández-Campos, Monitoring dexamethasone skin biodistribution with ex vivo MALDI-TOF mass spectrometry imaging and confocal Raman microscopy, *Int. J. Pharm.* 636 (2023) 122808, <https://doi.org/10.1016/j.ijpharm.2023.122808>.
- [43] A. Lee, D. Septiadi, P. Taladriz-Blanco, M. Almeida, L. Haeni, M. Spuch-Calvar, W. Abdussalam, B. Rothen-Rutishauser, A. Petri-Fink, Particle stiffness and surface topography determine macrophage-mediated removal of surface adsorbed particles, *Adv. Healthc. Mater.* 10 (2021) 2001667, <https://doi.org/10.1002/adhm.202001667>.
- [44] 2020, Microsphere-Based Drug Delivery to Alveolar Macrophages - a Review, *TJNPR* 4 (2020) 661–671. <https://doi.org/10.26538/tjnpr/v4i10.2>. 2020.
- [45] K.A. Beningo, Y. Wang, Fc-receptor-mediated phagocytosis is regulated by mechanical properties of the target, *J. Cell Sci.* 115 (2002) 849–856, <https://doi.org/10.1242/jcs.115.4.849>.
- [46] R. Rodríguez-Dorado, C. López-Iglesias, C. García-González, G. Auriemma, R. Aquino, P. Del Gaudio, Design of aerogels, cryogels and xerogels of alginate: effect of molecular weight, gelation conditions and drying method on particles' micromeritics, *Molecules* 24 (2019) 1049, <https://doi.org/10.3390/molecules24061049>.
- [47] M. Hosseinpour, A. Vatanara, R. Zarghami, Formation and characterization of beclomethasone dipropionate nanoparticles using rapid expansion of supercritical solution, *Adv. Pharm. Bull.* 5 (2015) 343–349, <https://doi.org/10.1517/apb.2015.048>.
- [48] J. Petitprez, F.-X. Legrand, C. Tams, J.D. Pipkin, V. Antle, M. Kfoury, S. Fourmentin, Huge solubility increase of poorly water-soluble pharmaceuticals by sulfobutylether- $\beta$ -cyclodextrin complexation in a low-melting mixture, *Environ. Chem. Lett.* 20 (2022) 1561–1568, <https://doi.org/10.1007/s10311-022-01415-y>.
- [49] Q.-Q. Xu, J.-Z. Yin, X.-L. Zhou, G.-Z. Yin, Y.-F. Liu, P. Cai, A.-Q. Wang, Impregnation of ionic liquids in mesoporous silica using supercritical carbon dioxide and co-solvent, *RSC Adv.* 6 (2016) 101079–101086, <https://doi.org/10.1039/C6RA20287J>.
- [50] P. Gurikov, I. Smirnova, Amorphization of drugs by adsorptive precipitation from supercritical solutions: a review, *J. Supercrit. Fluids* 132 (2018) 105–125, <https://doi.org/10.1016/j.supflu.2017.03.005>.
- [51] J. Feng, L. Fan, M. Zhang, M. Guo, An efficient amine-modified silica aerogel sorbent for CO<sub>2</sub> capture enhancement: facile synthesis, adsorption mechanism and kinetics, *Colloids Surf. A: Physicochem. Eng. Asp.* 656 (2023) 130510, <https://doi.org/10.1016/j.colsurfa.2022.130510>.
- [52] C.A. García-González, A. Sosnik, J. Kalmár, I. De Marco, C. Erkey, A. Concheiro, C. Alvarez-Lorenzo, Aerogels in drug delivery: from design to application, *J. Control. Release* 332 (2021) 40–63, <https://doi.org/10.1016/j.jconrel.2021.02.012>.
- [53] V. Santos-Rosales, B. Magariños, C. Alvarez-Lorenzo, C.A. García-González, Combined sterilization and fabrication of drug-loaded scaffolds using supercritical CO<sub>2</sub> technology, *Int. J. Pharm.* 612 (2022) 121362, <https://doi.org/10.1016/j.ijpharm.2021.121362>.
- [54] T. Riley, D. Christopher, J. Arrp, A. Casazza, A. Colombani, A. Cooper, M. Dey, J. Maas, J. Mitchell, M. Reiners, N. Sigari, T. Tougas, S. Lyapustina, Challenges with developing in vitro dissolution Tests for Orally Inhaled Products (OIPs), *AAPS PharmSciTech* 13 (2012) 978–989, <https://doi.org/10.1208/s12249-012-9822-3>.
- [55] F. Buttini, G. Brambilla, D. Copelli, V. Sisti, A.G. Balducci, R. Bettini, I. Pasquali, Effect of Flow Rate on In Vitro Aerodynamic Performance of NEXThaler® in Comparison with Diskus® and Turbuhaler® Dry Powder Inhalers, *J. Aerosol Med. Pulm. Drug Deliv.* 29 (2016) 167–178, <https://doi.org/10.1089/jamp.2015.1220>.
- [56] M.W. Jetzer, B.D. Morrical, M. Schneider, S. Edge, G. Imanidis, Probing the particulate microstructure of the aerodynamic particle size distribution of dry powder inhaler combination products, *Int. J. Pharm.* 538 (2018) 30–39, <https://doi.org/10.1016/j.ijpharm.2017.12.046>.

- [57] N. Bertho, F. Meurens, The pig as a medical model for acquired respiratory diseases and dysfunctions: an immunological perspective, *Mol. Immunol.* 135 (2021) 254–267, <https://doi.org/10.1016/j.molimm.2021.03.014>.
- [58] R.R. Mercer, M.L. Russell, V.L. Roggli, J.D. Crapo, Cell number and distribution in human and rat airways, *Am. J. Respir. Cell Mol. Biol.* 10 (1994) 613–624, <https://doi.org/10.1165/ajrcmb.10.6.8003339>.
- [59] A. Ananda Rao, S. Johny, Tennis courts in the human body: a review of the misleading metaphor in medical literature, *Cureus* (2022), <https://doi.org/10.7759/cureus.21474>.